

Analysis, design and performance of reinforced soil slopes in strong earthquakes

Michael Dobie

Asia Pacific Regional Manager, Tensar International Limited, Jakarta (tensar@attglobal.net).

ABSTRACT: Bishop's circular method of slices is outlined with adaptations to include the effects of both earthquake loading and geosynthetic reinforcement. Vertical and horizontal components of earthquake force may be included in the analysis, and may be attenuated by accepting that some deformation takes place. This is acceptable for slip circles in a reinforced soil slope which do not cut through layers of reinforcement. However in the case of circles which do cut through reinforcement, displacement on the sliding surface could imply rupture or excessive distortion of the reinforcement, so that full design acceleration should be used. For these circles, additional resisting force is provided by the layers of reinforcement, taking into account pull-out resistance and rupture strength, as well as fixity at the slope surface. For the polymers used to manufacture geosynthetic reinforcement, reduction factors must be used to take into account the long term effects of creep in static design. However during the short term increased loading due to earthquake shaking, there is no need to take creep into account, so that a higher short term strength value may be used without adverse effect on the long term capacity. The method of analysis described is used to analyse three large reinforced soil slopes which were affected by the 1999 Chi-Chi earthquake ($M_w = 7.6$) in Taiwan. One of these slopes failed and two did not fail. It is concluded that an adequately designed reinforced soil slope has excellent resistance to strong ground shaking during an earthquake, even when design ground accelerations are very high.

Keywords : slope stability, method of slices, earthquakes, geosynthetics, Chi-Chi

1 INTRODUCTION

The method of slices is used extensively to analyse and design soil slopes. Bishop's simplified method using a circular slip surface has the advantage of being easy to use, and the assumptions made do not lead to large inaccuracy. Also, from the point of view of design, routines may be set up in a number of ways to define slip circles (for example a grid of centres with varying radius) making it relatively easy to search for the minimum factor of safety, using a suitable computer program. The original method as described by Bishop (1955) does not include the effects of earthquakes and geosynthetic reinforcement, but the additional forces may be added to the simplified method by taking advantage of the simplifying assumptions used. In Section 2.0, Bishop's original method is outlined, then the effects of both earthquake loading and reinforcement are added. In Section 3.0, input parameters required to define both the stabilising effect of reinforcement and the destabilising effect of earthquake loading are discussed in detail.

In Section 4, the method of analysis outlined in Sections 2 and 3 is applied to three large reinforced soil slopes affected by the Chi-Chi earthquake which took place in central Taiwan in 1999. One of these slopes failed dramatically and has received much attention since, but the other two remained stable and were not significantly affected.

2 ANALYSIS OF SLOPE STABILITY USING METHOD OF SLICES

2.1 Outline of method of slices

Figure 1 illustrates the general formulation of the method of slices for analysing slope stability using a circular slip surface. The potentially failing soil mass above the surface is divided into a number of slices (total = N), and Slice “n” is shown on the figure. The sides of the slices need not be vertical, but they are in most methods of solution. The nomenclature used on Figure 1 is the same as used by Bishop (1955). The aim of stability analysis is to find a set of boundary forces which keep the soil mass in equilibrium.

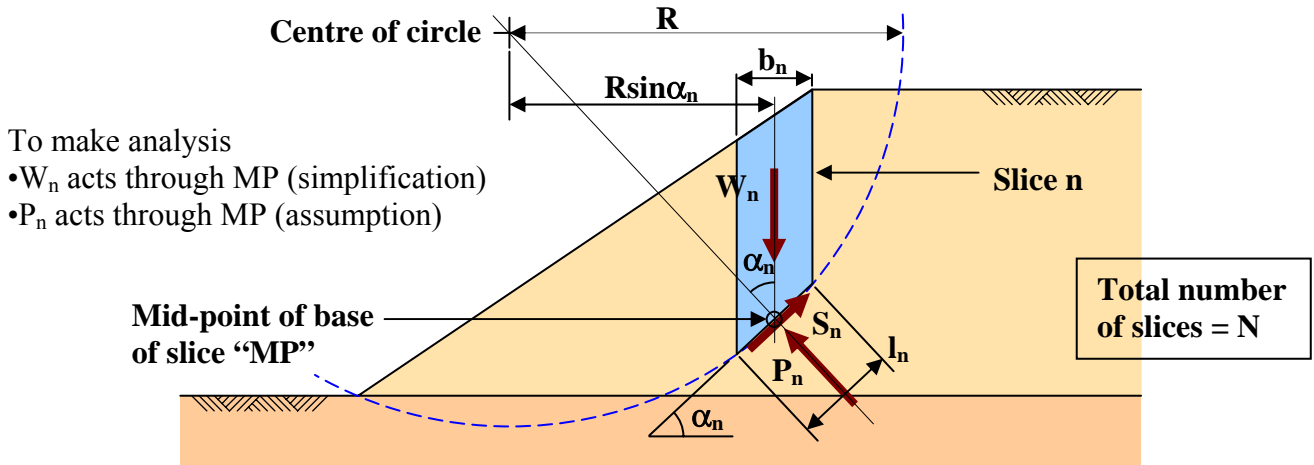


Figure 1. General formulation of the method of slices.

In the case of the circular slip surface, a convenient method of assessing overall stability of the soil mass is to take moments about the centre of the circle. As shown, the external forces acting on each slice consist of the slice weight (W_n), the normal force on the base (P_n) and the shear force on the base (S_n). It is necessary to make the assumption that P_n acts through the mid point of the base of the slice (MP) and the simplification that W_n also acts through MP. Taking moments about the centre of the circle, we can then say for Slice n:

$$\text{Disturbing moment} = W_n R \sin \alpha_n$$

$$\text{Resisting moment} = R S_n$$

P_n has no moment (it acts through the centre of the circle)

If we sum the moments, then for limiting equilibrium:

$$\sum W_n R \sin \alpha_n = \sum R S_n$$

S_n is unknown. It is possible to cancel R from each side of this equation, but in this formulation it will be retained, which is necessary when earthquake forces and geogrid reinforcement are introduced.

A simple solution to this equation may be found for cases where soil shear strength is defined by the undrained shear strength (s_u). In this situation, S_n is given as:

$$S_n = l_n s_u / F \text{ (where } F \text{ is the safety factor so that } S_n \text{ is then the mobilised or available shear strength)}$$

$$S_n = b_n s_u \sec \alpha_n / F \text{ (defining the slice width in terms of the horizontal width, } b_n \text{)}$$

This expression for S_n may be substituted into the equation above, and rearranged to give an expression for the overall safety factor of the slope:

$$F = \frac{R \sum b_n s_u \sec \alpha_n}{R \sum W_n \sin \alpha_n}$$

This equation gives a rigorous solution for the factor of safety (F) where the soil shear strength is defined in terms of the undrained shear strength only, and the analysis is carried out in terms of total stress. However for most slope stability analyses it is necessary to define shear strength in terms of the drained parameters c' and ϕ' , and therefore stresses must be calculated in terms of effective stress. This is outlined in the next section, following the technique developed by Bishop (1955).

2.2 Bishop's method of slices for circular slip surfaces

The Mohr Coulomb equation defines shear strength (s) in terms of the parameters c' and ϕ' in the form:

$$s = c' + (\sigma - u)\tan\phi'$$

where σ is the total effective stress on the shear plane and u is the pore water pressure

In order to utilise this definition of shear strength in the method of slices, it is necessary to take all forces applied to the slice into account including the forces on the internal boundaries of the slice, referred to as the "inter-slice" normal and shear forces (E_n and X_n). This is illustrated on Figure 2. Different formulations use different techniques, but in the method developed by Bishop (1955) this is done by resolving the forces vertically. This vertical resolution of forces means that the normal inter-slice forces (E_n) are eliminated, and a solution for S_n may be found. The full derivation is given by Bishop (1955) and will not be repeated here. However these principles are important because they are relevant to the inclusion of both earthquake forces and geogrid reinforcement, which will be examined in the next following sections. The resulting well known formula (including the R term) is given below:

$$F = \frac{R \sum [c'_n b_n + (W_n + DX_n - ub_n) \tan \phi'_n] \left[\frac{\sec \alpha_n}{1 + \frac{\tan \phi'_n \tan \alpha_n}{F}} \right]}{R \sum W_n \sin \alpha_n}$$

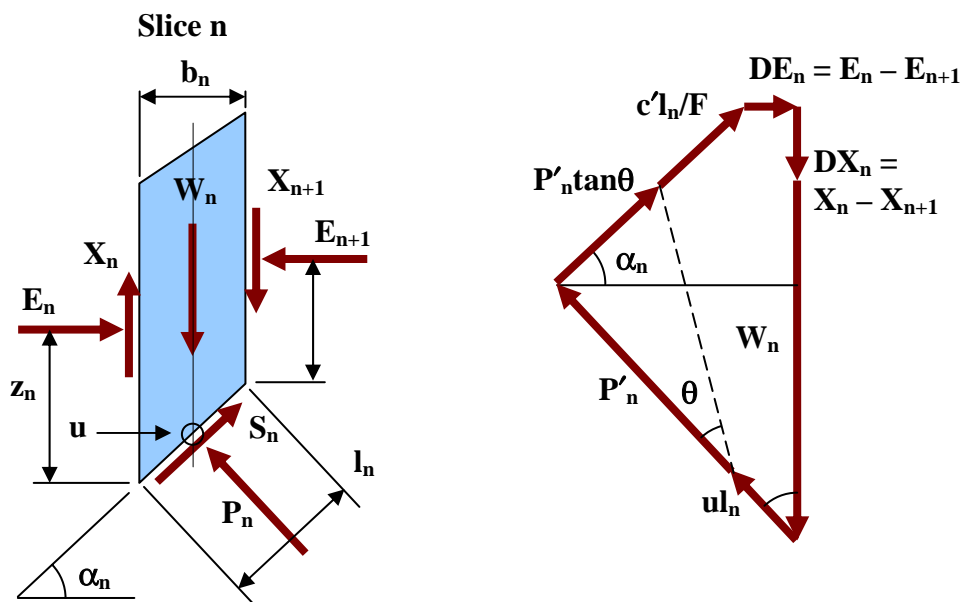


Figure 2. Definition of all forces applied to Slice "n".

It is important to realise that, although the E_n forces have been eliminated, they are still present and may be found by horizontal resolution of forces on the individual slices. In order to solve this equation, it is necessary to assume a distribution of the inter-slice shear forces (X_n), then calculate F by iteration (it appears on both sides of the equation). Once F has been found, it is then necessary to check that all the internal forces are physically acceptable (eg. P_n and E_n are positive and act at a reasonable location, and X_n forces do not violate the failure criterion). This will inevitably lead to adjustments in the assumed distribution of X_n forces being required and repeated a number of times, until a satisfactory rigorous solution is found. This is a very laborious process, and is not suitable for regular use.

Bishop (1955) also established a "routine" method to make the solution of this equation easier, by assuming that the $DX_n = X_n - X_{n+1}$ forces are zero for each slice. In this case it is only necessary to iterate to find F , and the method is normally referred to as *Bishop's Simplified Method of Slices* (although it should be noted that in his paper, Bishop refers to the USBR or Ordinary method as the "simplified method"). It should be noted that the resulting E_n and S_n forces, which may be derived by analysing the internal forces following the simplified solution, are likely to have significant errors for any particular slice, however over the full N slices these errors tend to cancel out. Bishop (1955) showed that the difference in the calculated value of F between the rigorous and routine solutions was between 1% and 2% in a typical dry slope (slightly higher for a partially submerged slope under rapid drawdown), therefore quite acceptable. However this conclusion was only reached based on analysing relatively low angle soil slopes, and the effects of earthquake loads and geosynthetic reinforcement were not examined.

2.3 Adding earthquake forces to Bishop's simplified of method of slices

In establishing techniques for incorporating additional load components into Bishop's simplified method of slices, based on circular slip surfaces, it is easier to consider the equation as follows:

$$F = \frac{R \sum m}{R \sum W_n \sin \alpha_n}$$

which is derived from the *external moment equilibrium* of the soil mass about the centre of the circle

$$\text{where } m = [c'b_n + (W_n - ub_n) \tan \phi'] \left[\frac{\sec \alpha_n}{1 + \frac{\tan \phi' \tan \alpha_n}{F}} \right] = S_n F$$

which is derived from *vertical resolution of internal forces* on each individual slice.

In this case "m" is the total ultimate shear resistance on the base of each slice, but it must be remembered that it includes F, but it is a secondary effect, hence allowing the iteration for F to converge. Figure 3 shows the forces applied to Slice "n" to model loading applied during an earthquake (h_n is the height of each slice at its mid-point). This is normally referred to as pseudo-static analysis, because the transient additional loads created by the earthquake are modelled as static loads. In Figure 3, both horizontal and vertical components of the earthquake load are shown (represented by k_h and k_v where k is the proportion of the vertical acceleration due to gravity, g).

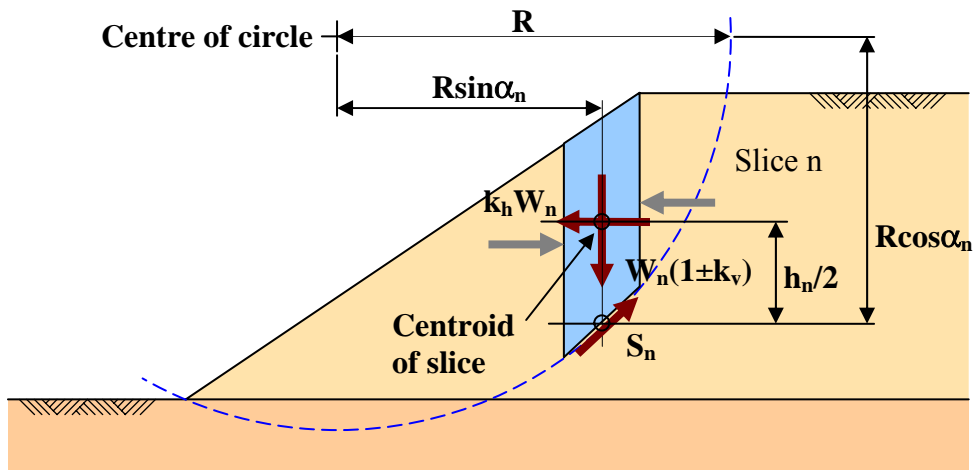


Figure 3. Additional forces applied to Slice "n" by earthquake (pseudo-static analysis).

Based on Figure 3, it is relatively straightforward to add the additional external forces to the external moment equilibrium of the sliding mass, to give:

$$F = \frac{R \sum m}{R \sum W_n (1 \pm k_v) \sin \alpha_n + \sum k_h W_n (R \cos \alpha_n - h_n / 2)}$$

As regards the equilibrium of each slice to find "m", the additional forces due to the earthquake must be considered. In Bishop's simplified method the sum of the additional shear forces on the slice boundaries are assumed to be zero ($\sum DX_n = 0$, and are not shown on Figure 3). However there are various components of horizontal force ($k_h W_n$ as well as additional horizontal forces on the slice boundaries), but due to Bishop's method of resolving internal forces vertically, these are all eliminated and do not affect the expression for "m" given above. However the vertical component of the earthquake force does affect "m", which becomes:

$$m = [c'b_n + (W_n (1 \pm k_v) - ub_n) \tan \phi'] \left[\frac{\sec \alpha_n}{1 + \frac{\tan \phi' \tan \alpha_n}{F}} \right]$$

In cases where the base of the slice is located above the phreatic surface, and $u = 0$ is assumed, then "m" is calculated as given above. However if pore water pressures are present, then the soil is assumed to be saturated, so that the change in weight due to the vertical acceleration is an undrained loading, resulting in a change in pore water pressure which could be entered into the equation. This change in pore pressure will be the same as the change in total vertical stress, so that the effective stress remains unchanged and the net effect of k_v is zero. Therefore k_v may simply be neglected in the calculation of "m" (McCombie, 2006), and due to

the very short duration of loading during an earthquake it would apply to all soil types. The vertical acceleration k_v is still applied in the denominator of the expression for F above, whether above or below the phreatic surface.

In the paper by Bishop (1955), a simple method is given for taking into account submergence, where buoyant weight is used for the portion of each slice below the level of the external water, and pore water pressure is then calculated as being the height of the phreatic surface above this level only. It is important to note that the earthquake accelerations k_h and k_v should be applied to the total weight of each slice, both above and below the level of the external water in deriving the overall moment equilibrium. For “ m ” the arguments given in the previous paragraph are always relevant (in the case of partial submergence), and k_v is not applied.

2.4 Adding the stabilising effect of geosynthetic reinforcement to Bishop’s simplified method of slices

In slopes where geosynthetic reinforcement is used to improve stability, the contribution may be modelled by the additional forces provided by the reinforcement, both at the inter-slice boundaries (internal forces) and where reinforcement is cut by the circular slip surface which contributes directly to the stability (external forces). These forces are shown on Figure 4.

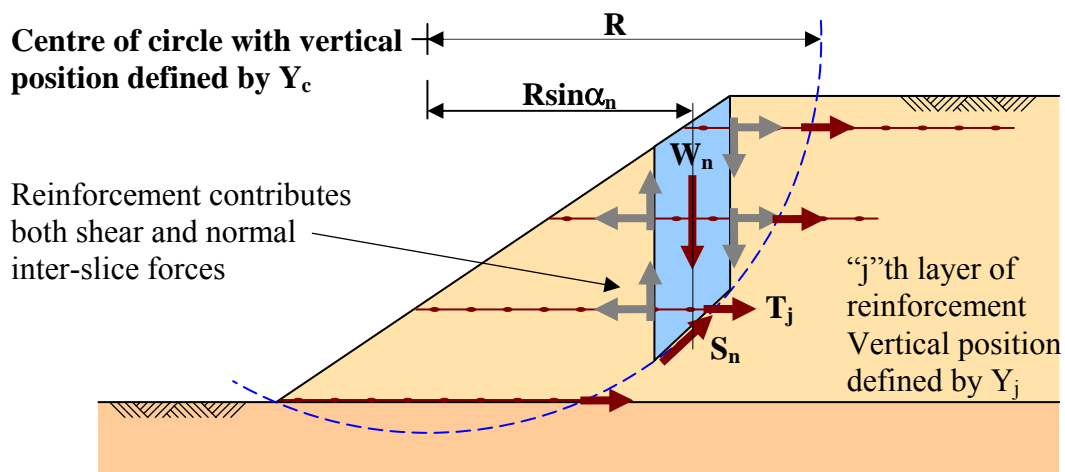


Figure 4. Additional forces applied to Slice “ n ” and the soil mass by geosynthetic reinforcement.

In Figure 4, the vertical position of each layer of reinforcement is defined by its Y coordinate (Y_j for layer “ j ”). The maximum available force is given by T_j so that the available moment of each layer of reinforcement is given by $T_j(Y_c - Y_j)/F$, where F is the required overall factor of safety. If the moment contribution of each layer of reinforcement is summed, and then added to the external stability equation, the resulting factor of safety of given by:

$$F = \frac{R \sum m + \sum T_j (Y_c - Y_j)}{R \sum W_n \sin \alpha_n}$$

As regards the contribution to the internal stability of each slice, inter-slice forces are generated where the reinforcement cuts the vertical slice boundary. However, as with the earthquake forces, the assumptions used in Bishop’s simplified method may be applied, so that the difference between the additional shear forces on the slice boundaries (DX_n) are assumed to be zero. There are additional normal forces, which are the mobilised tensile forces from the reinforcement and may be included in the polygon of forces (as in Figure 2). However, but by resolving internal forces vertically, these are all eliminated and do not affect the expression for “ m ” given previously.

3 PARAMETERS USED IN ANALYSIS OF SLOPE STABILITY

3.1 Resistance from geosynthetic reinforcement under static loading

The value of T_j at each level is the available resistance from the reinforcement at the point where it is cut by the slip circle. The value may be given by any of:

- Pull-out from the buried end (calculated by a pull-out relationship)
- Rupture of the reinforcement (calculated from the strength of the reinforcement)
- Pull-out from the facing (calculated by a pull-out relationship for a “free end”)

The resistance defined by these three failure criteria may be calculated at any point along the reinforcement, and the appropriate resistance value to be used is the lowest of the three. This is best modelled or visualised as an *envelope of available resistance* from the reinforcement, as shown in Figure 5. The normal definitions of pull-out resistance and reinforcement strength under static loading are given by:

$$\text{Pull-out resistance} = \sum 2\alpha_p(c' + \sigma'_v \tan\phi')\delta x \quad [\text{summation of } \sigma'_v \times \alpha_p \text{ over the anchorage length}]$$

$$\text{Reinforcement strength} = P_{des} = T_{ult}/(RF_{CR} \times RF_M \times RF_{ID} \times RF_D)$$

- Where
- x = distance along reinforcement measured from the end
 - α_p = pull-out interaction factor
 - c' = cohesion intercept in terms of effective stress
 - ϕ' = frictional strength in terms of effective stress
 - σ'_v = vertical effective stress
 - T_{ult} = ultimate tensile strength (based on short term test)
 - RF_{CR} = reduction factor for creep (long term performance)
 - RF_M = reduction factor for manufacturing variation and data extrapolation
 - RF_{ID} = reduction factor for installation damage
 - RF_D = reduction factor related to environmental durability

The distribution shown on Figure 5 assumes that the reinforcement is not fixed to any form of facing, a condition referred to as “free”. This is normally the case for low angle slopes as shown in Figure 6, so that shallow circles can generate resistance controlled by pull-out from the facing. For steeper structures where the reinforcement is likely to be connected to the facing, the tensile strength (P_{des}) may be generated all the way to the facing (shown as the dotted area on Figure 5). This condition is referred to as “fixed”.

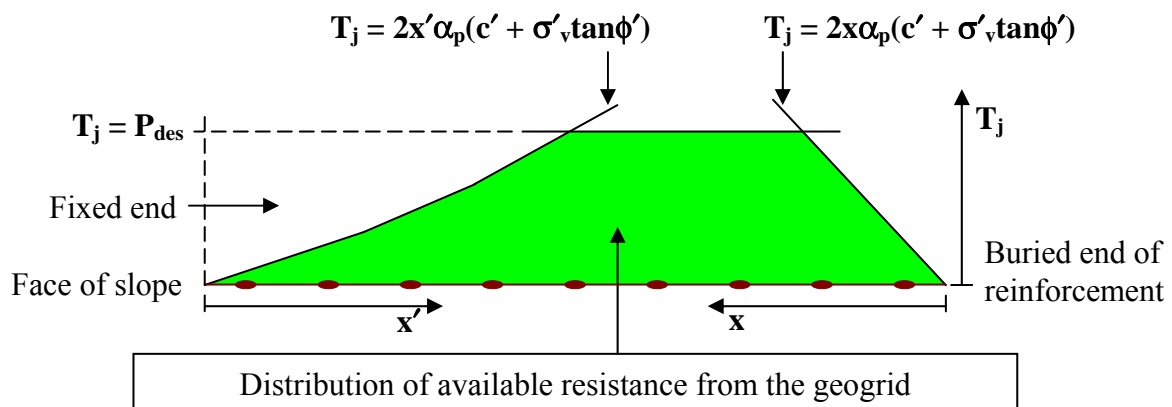


Figure 5. Envelope of available resistance from a layer of geosynthetic reinforcement.

The application of these envelopes of resistance is illustrated on Figure 6. For this low angle slope there is no connection to the facing so that the end condition is “free”. Two circles are shown. In the case of Circle 1, it cuts all four layers of reinforcement, with the lower two layers generating full design strength. The third layer has a pull-out failure from the buried end, whereas the top layer pulls out from the facing. In the case of Circle 2, the shallow failure through the two layers of reinforcement results in pull-out from the facing.

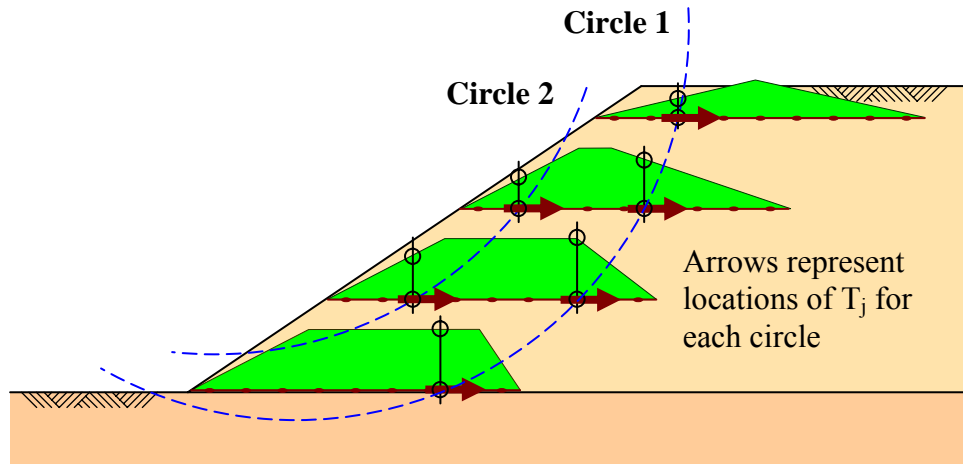


Figure 6. Examples of circles showing resistance from layers of geosynthetic reinforcement.

3.2 Resistance from geosynthetic reinforcement under earthquake loading

The additional forces applied to geosynthetic reinforcement during earthquake shaking are transient and of short duration. This affects the definitions both of pull-out resistance and of reinforcement strength, which become:

$$\text{Pull-out resistance} = \sum 2\alpha_p [c' + \sigma'_v(1 \pm k_v)\tan\phi'] \delta x$$

$$\text{Reinforcement strength} = P_{\text{des}} = T_{\text{ult}} / (\text{RF}_M \times \text{RF}_{\text{ID}} \times \text{RF}_D)$$

In the case of pull-out, the vertical effective stress on the geogrid used to calculate the frictional component of resistance is modified by the vertical acceleration, however as with the “m” component in Section 2.3, it is only applied if the reinforcement is located above the phreatic surface, and omitted if it is located below it. It can be seen that upward vertical acceleration will reduce pull-out resistance, so may well result in a more critical stability condition than downward vertical acceleration. But because other components of force will also be affected by k_v it is not certain whether k_v (up) or k_v (down) will be critical, so both should be checked for each potential slip circle.

In the case of reinforcement strength, the short term nature of earthquake loading has a significant effect on the resistance available. Geosynthetic reinforcement (normally made from either high density polyethylene HDPE or polyester PET) is visco-elastic. Under short term loading both strength and stiffness are significantly higher than under a long term sustained load. This is shown on Figure 7 for an HDPE geogrid, where the lower line is the isochronous load-strain behaviour at 120 years, the typical design life for many reinforced soil structures. However the peak accelerations during an earthquake only last for a fraction of a second, and under such short term loading, the load-strain “curve” would fall well above the 120 year isochronous behaviour. In the NCMA Seismic Design Manual (Bathurst, 1998), the simple recommendation is to use the short term tensile strength of the geogrid (T_{ult}) to resist earthquake loads (adjusted by partial material factors as shown above). This test is normally used for quality control purposes, and the normal standard (ISO10319:1996) uses a strain rate of 20% per minute, so would typically be completed in about 30 seconds - far longer than the duration of a peak “pulse” of load from an earthquake. Therefore although the use of T_{ult} may well be conservative, the data is readily available, so easily applied for earthquake design.

In Figure 7, the difference between the 120 year isochronous curve and the tensile test may be considered as a “reserve” of strength available to resist short term loads, such as earthquake loading, while the long term back-ground loading is resisted by the isochronous curve alone. The magnitude of this reserve is considerably larger for HDPE reinforcement than for PET. This concept is explored in far more depth by McGown (2000) in the 2000 Mercer Lecture, in terms of isochronous strain energy, concluding that very short term loading up to T_{ult}/F does not have an adverse effect on the long term strength of the reinforcement under sustained loading.

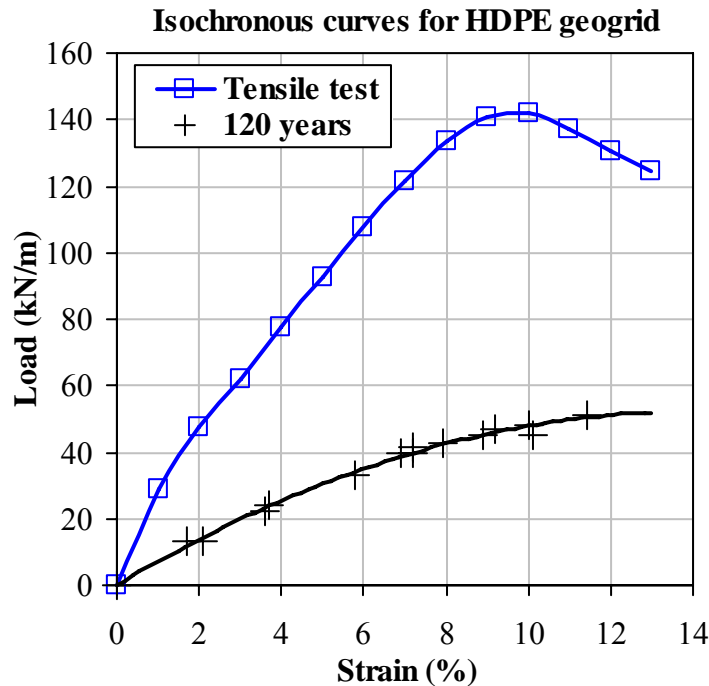


Figure 7. Comparison of short term tensile strength behaviour with 120 year isochronous curve for HDPE reinforcement.

The result of this method of assessing the available resistance from geosynthetic reinforcement during earthquake shaking may still be visualised in terms of an envelope, but with reference to Figure 5, the envelope will be considerably higher than for the static case due to the higher short term reinforcement strength, but the slopes representing pull-out may be at a lower angle if k_v is acting upwards.

3.3 Definition of earthquake acceleration parameters

The input parameter used to represent earthquake shaking is acceleration, normally given as a proportion of the acceleration due to gravity, (ie 0.25g denotes an acceleration equivalent to 25% of gravity). Values suitable at any particular site are either taken from suitable building or engineering codes, or derived from seismic hazard analysis. In most cases this is defined as the *peak ground acceleration*, “A”. For design of buildings it is normally necessary to amplify or attenuate A, depending on the natural period of the structure being designed. However for soil structures, the peak ground acceleration is generally used directly as the input acceleration at the base of the structure. In many codes, this is limited to a horizontal component only, A_h , but depending on the nature of the tectonic movements creating the earthquake, the vertical component, A_v , may also be significant. Vertical acceleration may easily be included in slope stability analysis as outlined in Section 2.3, and should be considered acting both upwards and downwards for all circles checked.

Soil structures reinforced with geosynthetic materials are highly ductile, and can absorb the energy created by seismic shaking very effectively. The pseudo-static design method cannot model this ductility satisfactorily, especially when accelerations become relatively large. In the adaptation of the method of slices described here, modelling of peak ground acceleration for design is based on recommendations given in the FHWA design guide for reinforced soil structures (Elias et al, 2001), which permits attenuation on the assumption that some deformation is tolerable. Section 6.3e of the guide states: “Reinforced slopes are flexible structures and unless used for bridge abutments they are not laterally restrained. Thus it is appropriate to use $A_m = A/2$ for seismic design in accordance with the AASHTO code. A_m is equivalent to the horizontal seismic coefficient k_h used in many slope stability programs.” This approach may be explained by examining Figure 8, which shows a typical acceleration record for a strong earthquake. In this case there are two acceleration peaks where the ground acceleration exceeds 0.2g (the chosen design acceleration) for short periods. Displacement will take place during these periods, but it will be relatively small due to the short durations involved. There will be some lag between the underlying ground accelerations and those experienced by the relatively steep reinforced slope, such that the full acceleration may not be experienced. Also, when the peak acceleration is experienced in an unfavourable direction, it will always be immediately followed by a substantial acceleration in the opposite direction, tending to arrest any movement that might take place.

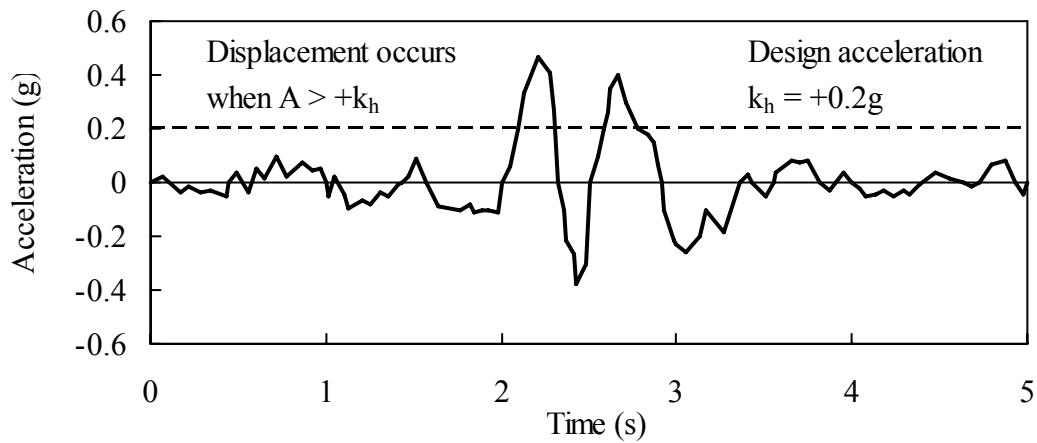


Figure 8. Record of acceleration against time during seismic shaking.

This simple approach is considered acceptable for peak ground accelerations up to 0.29g according to the AASHTO/FHWA design guideline (0.4g in the NCMA seismic design guide, Bathurst, 1998), and above this is likely to become either unreliable or over-conservative. FHWA also recommends that a lower target factor of safety is acceptable (1.1 for seismic, compared to 1.3 recommended for static conditions). For accelerations above 0.29g, it is recommended that the pseudo-static method is used with caution, and it may be necessary to use a full dynamic analysis in such cases, or certainly make an assessment of likely deformations.

Likely deformations may be assessed using the Newmark sliding block displacement method as described by Cai and Bathurst (1996). However an indication of likely displacement is given by Wood and Elms (1990), by the expression:

$$d = \frac{3v^2}{Ag} \left[\frac{A}{k_h} + \frac{k_h}{A} - 2 \right]$$

- where
- d = Displacement
 - v = peak ground velocity $\approx 1.3A$ m/s
 - A = peak ground acceleration coefficient
 - g = acceleration due to gravity
 - k_h = Horizontal design acceleration coefficient

This reduces to the following expression:

$$d = 517A \left[\frac{A}{k_h} + \frac{k_h}{A} - 2 \right] \text{ in mm}$$

where A is given as a fraction of the acceleration due to gravity. The resulting displacements predicted for varying values of k_h/A are as follows in Table 1:

k_h/A	d (mm)	d (mm) for A = 0.4g	k_h/A	d (mm)	d (mm) for A = 0.4g
1	0	0	0.6	138A	55
0.9	6A	2	0.5	258A	104
0.8	26A	10	0.4	465A	186
0.7	66A	27	0.3	844A	338

Table 1 Approximate displacements based on k_h/A .

For the case of $k_h = 0.5A$, as recommended for design by AASHTO/FHWA, the likely displacement will be in the order of 258A mm. This magnitude of likely displacement is given both in the AASHTO/FHWA design guides and the NCMA seismic design guide. An important and logical point made by Wood and Elms (1990) is that, if deformation is assumed to take place during an earthquake, then the critical acceleration (k_h) should be calculated using the maintainable shearing resistance of the soil at large strains.

In assessing design acceleration parameters, one further important point should be considered, as outlined in the NCMA seismic design manual by Bathurst (1998). The attenuation of peak ground acceleration, as outlined above, is acceptable in the case of failure mechanisms which do not cut through geosynthetic

reinforcement, such as slip circles outside the reinforced soil block, or which are located between layers of reinforcement. But in all mechanisms which cut through reinforcement layers (for example the two circles shown on Figure 6) it would not be acceptable to permit large displacements because this would result in either rupture or extensive distortion of the reinforcement. In the case of retaining walls, it is recommended that the peak ground accelerations are amplified [$k_h = (1.45 - A_h)A_h$] for any internal failure mechanisms which cut through reinforcement, however for lower angle slopes, it is considered adequate to use the full peak ground acceleration, so that $k_h = A$.

Based on the discussion given above, the following recommendations are given for assessing the acceleration parameters to be used in the method of slides applied to reinforced soil slopes when earthquake loads are included:

Mechanism	Design acceleration
Slip circles outside the reinforced soil block, as well as any internal circles which do not cut through geosynthetic reinforcement	$k_h(\text{ext}) = 0.5 A_h$ $k_v(\text{ext}) = 0.5 A_v$
All slip circles which do cut through geosynthetic reinforcement	$k_h(\text{int}) = A_h$ $k_v(\text{int}) = A_v$

4 APPLICATION OF THE METHOD TO THREE REINFORCED SOIL SLOPES

4.1 Summary of the method

The full formulation of Bishop's routine (simplified) method of slices taking account of partial submergence, and adapted to include earthquake forces and geosynthetic reinforcement is:

$$F = \frac{R \sum [c' b_n + (W_n (1 \pm k_v) - W_{sn} - u_s b_n) \tan \phi'] \left[\frac{\sec \alpha_n}{1 + \frac{\tan \phi' \tan \alpha_n}{F}} \right] + \sum T_j (Y_c - Y_j)}{R \sum (W_n (1 \pm k_v) - W_{sn}) \sin \alpha_n + \sum k_h W_n (R \cos \alpha_n - h_n / 2)}$$

The terms and parameters have all been defined and discussed in Sections 2 and 3 of this paper, except W_{sn} which is the weight of water displaced by the slice below the level of external water in the case of partial submergence, and u_s which is pore water pressure associated with each slice, but calculated as the height of the phreatic surface above the level of any external water. In the case of slopes without partial submergence, W_{sn} is not required, and u_s becomes u , the pore water pressure at the base of the slice.

Tensar International have developed a slope stability computer program, called "Winslope" (McCombie, 2006) which includes the formulation of Bishop's simplified method of slices as given above. The various parameters discussed in Section 3 are included in the input into the program. This program has been used to analyse the stability of three large reinforced soil slopes affected by the Chi-Chi earthquake, which caused severe damage in central Taiwan in 1999.

4.2 The Chi-Chi earthquake

The Chi-Chi earthquake occurred in the early hours of 21st September 1999 resulting from rupture along the Chelungpu fault in central Taiwan. The moment magnitude of the main shock was $M_w = 7.6$. The motions generated by the main shock of this earthquake were recorded at 387 strong motion stations, which are shown on Figure 9, and distinguished by the dominant soil type at each location, from soft soil to rock or rock-like. Idriss and Abrahamson (2000) give a good summary of the strong motion data recorded, and Figure 9 is taken from their paper. They also plot the measured peak horizontal ground accelerations against distance from the fault break, as shown on Figure 10. This figure shows the attenuation of peak ground acceleration with distance from the fault break, and it can be seen that as far as 40 km from the fault break $A_h = 0.4g$ was measured. It is also important to note that the higher peak ground accelerations were only recorded at the firmer soil sites.

Further information concerning the measured ground motion parameters is given in Figure 11. This shows the relationship of peak vertical ground acceleration to peak horizontal ground acceleration measured at several strong motion monitoring stations. Almost everywhere the horizontal acceleration is greater than the

vertical component, but the vertical component is significant, with the mean ratio being greater than 0.5. This may well be related to the nature of the tectonic plate movements in the case of the Chi-Chi earthquake (the plate boundary in this area is a zone of subduction), which tended to encourage a significant vertical component of movement (and therefore acceleration) on the fault plane.

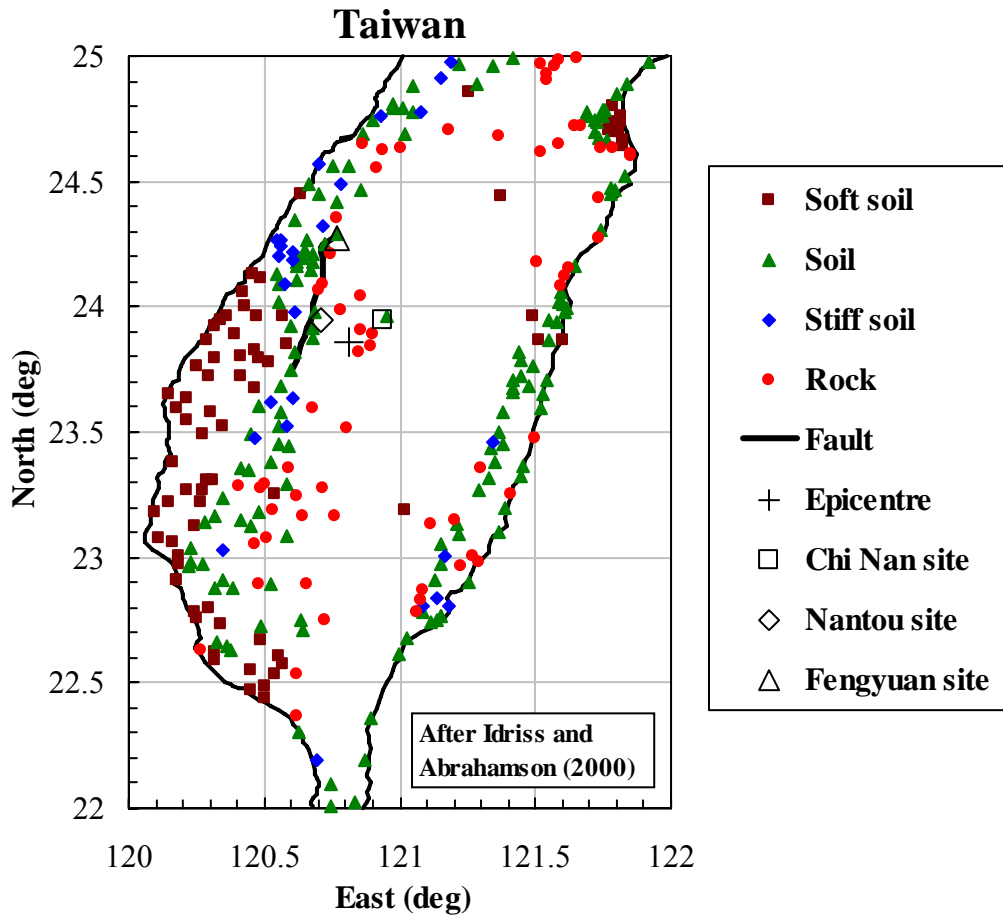


Figure 9. Taiwan showing Chi Chi earthquake epicenter, fault break, measurement locations and slope sites.

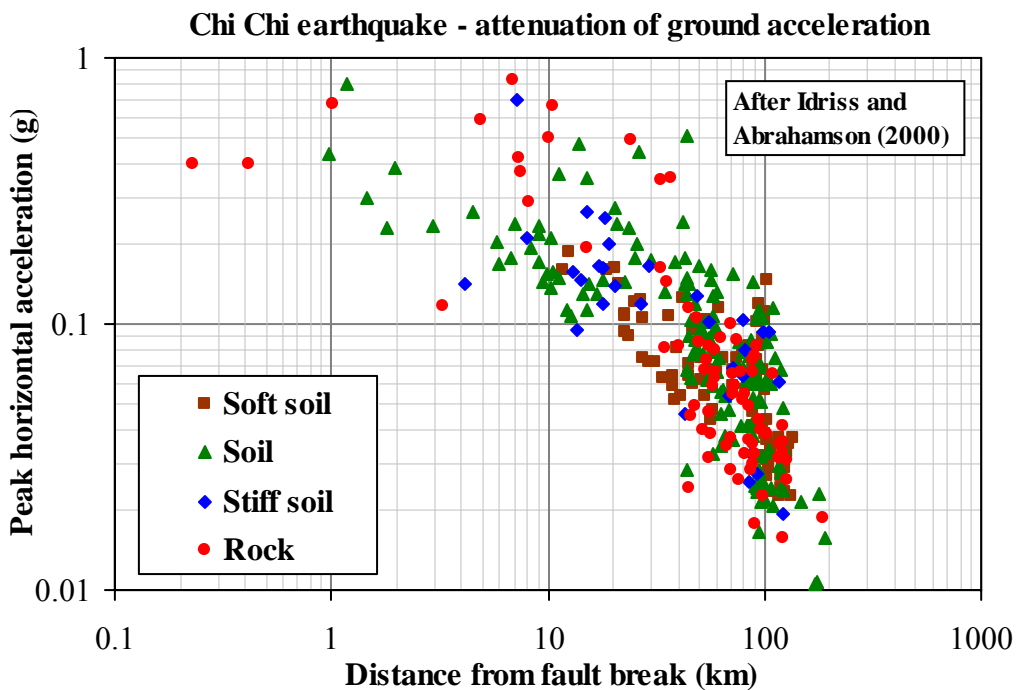


Figure 10. Chi Chi earthquake: attenuation of peak horizontal ground acceleration related to foundation soil type.

Figure 9 shows the location of the earthquake epicentre, as well as the surface fault break which runs for about 80km in a mainly north-south direction. The map also shows the locations of three large reinforced soil slopes, all situated quite close to the fault break. The three sites are referred to as:

- Fengyuan (repair of a slope failure below a golf course near Fengyuan)
- Nantou (construction of a steep slope as part of a housing project)
- Chi-Nan (reinforced soil slope forming access to National Chi-Nan University)

The author visited all three slopes soon after the earthquake occurred. Of the three slopes, the Chi-Nan slope failed dramatically during the Chi-Chi earthquake and has received much attention since (for example Holtz et al, 2001). The other two slopes performed very well, with no visible signs of significant distress, despite being much closer to the fault break (although Fengyuan is quite a lot further away from the earthquake epicentre than the other two). Each slope is assessed below, using Bishop's simplified method of slices modified as described in Sections 2 and 3 of this paper, using the program "Winslope". The Chi-Nan failure mechanism was almost certainly not a circular arc, but the aim of these analyses is to examine whether or not the observed performance could have been expected based on routine design calculations.

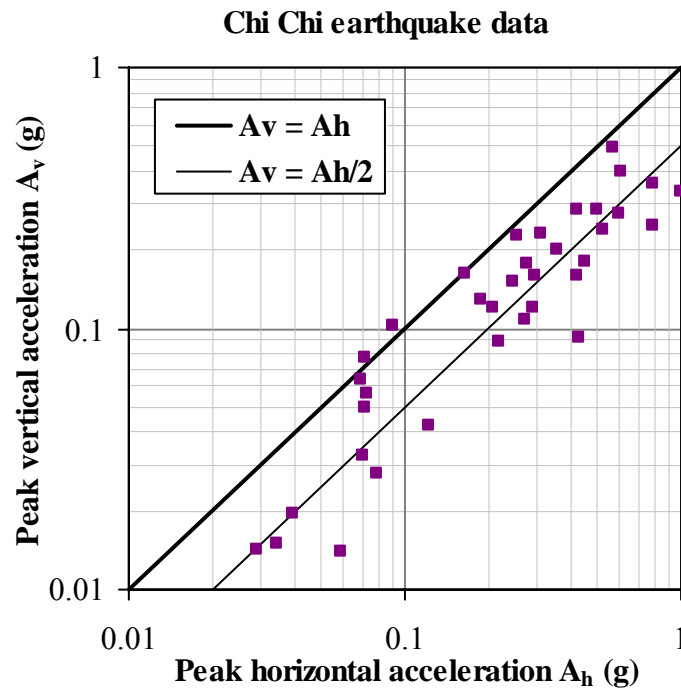


Figure 11. Chi Chi earthquake: relationship of peak horizontal and vertical ground acceleration.

4.3 Slope at Fengyuan

The slope at Fengyuan is situated a few kilometres from the fault break, not far from the location where the maximum vertical displacement of the surface rupture was observed. However it is quite far from the earthquake epicentre (about 46 km). With reference to Figure 4, peak horizontal ground acceleration could easily have been in the order of 0.3 to 0.4g, and the golf course above the slope suffered many slope failures at other locations due to the earthquake. The original purpose of this slope was to repair a failure in a valley leading down from the golf course, and it was constructed in 1995.

A typical cross section of the slope is shown on Figure 12. The slip repair consists of a lower reinforced section of between 15 and 20m height, with face angle 0.5:1 and 2.5m wide benches every 5m. The upper section is unreinforced with a face angle of 1.5:1 and 1.5m wide benches every 5m. The fills forming the slopes were well benched into the existing slope surface after removing the slip debris. The fill soils used for the construction were locally won, consisting of weathered silty sandstone. In the analysis, parameters used for the fill soils were $\phi' = 35^\circ$, $c' = 5$ kPa and $\gamma = 20$ kN/m³. The properties of the in-situ soils below the fills are slightly better. The slope is reinforced with HDPE geogrid, consisting of two grades with tensile strengths of 136 kN/m and 173 kN/m, at a uniform vertical spacing of 0.5m.

The original design of this slope was carried out using Winslope, but further stability analyses have been carried out using the same program, and the results are summarised in Table 2. Circles were defined by

fixing the exit point at each bench level (indicated on Figure 12), then letting the location of the circle centre vary until minimum factor of safety was found. Therefore circles defined by Bench 1 only intersect the upper unreinforced slope, whereas the other benches involve varying amounts of reinforcement. The sensitivity of the results to peak ground acceleration is examined by looking at varying values of A_h both with and without an A_v component, up to the recommended limit for pseudo-static analysis of 0.4g.

Bench	Static	$A_h = 0.15g$ $A_v = 0.15g$	$A_h = 0.3g$	$A_h = 0.3g$ $A_v = 0.15g$	$A_h = 0.4g$
1	1.517	1.180	0.928	0.883	0.793
2	1.983	1.484	1.163	1.135	1.007
3	2.106	1.560	1.248	1.187	1.080
4	1.954	1.456	1.170	1.114	1.015
Base	1.914	1.436	1.157	1.097	1.006

Table 2 Minimum factors of safety calculated for the Fengyuan slope for varying peak ground accelerations.

It is believed that the slope was originally designed with $A_h = A_v = 0.15g$, suggesting that that the initial design might have been somewhat conservative, however at the time of design, some of the features described in Section 3 were not included in Winslope, in particular using $k = A/2$ for external circles and using the short term tensile strength T_{ult} for the geogrid design strength during earthquake loading (both these features of the program at the time would have lead to more conservative designs). From this analysis it can be seen that the upper slope generally has a lower factor of safety. For the reinforced slope, critical peak ground acceleration (ie ground acceleration resulting in $F = 1.0$) is around $A_h = 0.4g$, or possibly $A_h = 0.3g$ with a vertical component of 50% of this. An approach using either peak horizontal acceleration only or a combination of a lower value of peak horizontal with a vertical component (it is very unlikely that peak vertical and peak horizontal ground accelerations will act at exactly the same moment in time) would appear to be sensible.

The slope at Fengyuan survived the Chi-Chi earthquake with minimal damage (some minor deformations and cracking of drains could be seen at the top of the slope), and the analysis outlined above compared to the likely level of ground motions suggested on Figure 10 indicate that this could have been expected based on routine stability analysis.

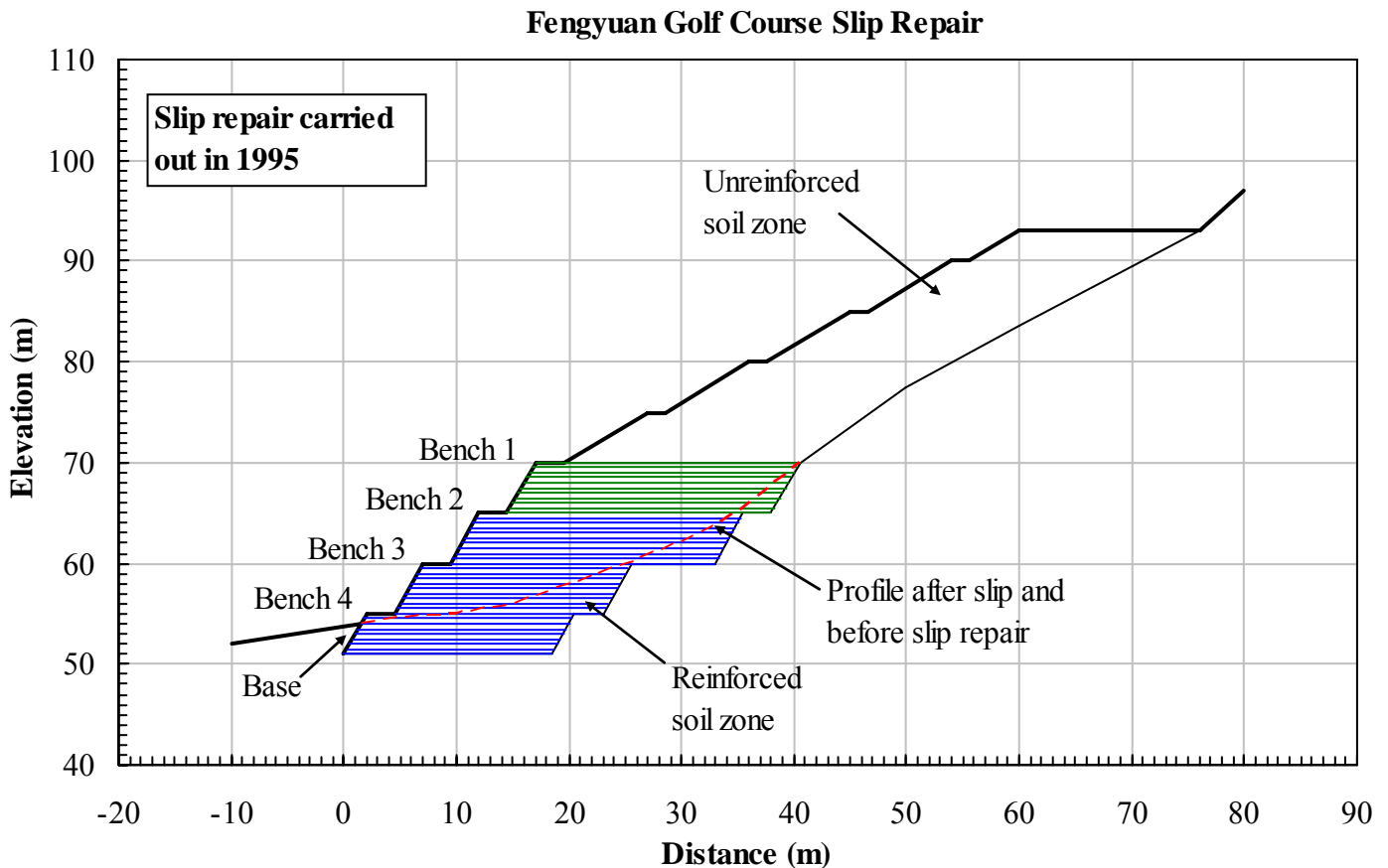


Figure 12. Typical cross section of the Fengyuan reinforced soil slope.

4.4 Slope at Nantou

The slope at Nantou is situated a few kilometres from the fault break, and is also quite close to the epicentre, about 15 km away. Details concerning the design and construction of the slope are reported by Chao et al (1994). The slope was built in 1993, and its purpose was to create level platforms for a housing development. At the time of the Chi-Chi earthquake in 1999, no houses had been built above the slope.

A typical cross section of the slope is shown on Figure 13. The reinforced section is 30m high with face angle 0.5:1 and 2.5m wide benches every 5m. There are small unreinforced benches on the top giving an overall height of about 35m. The fill soils used for the construction are described as weathered shale. Parameters given for the fill in the published paper are $\phi' = 29^\circ$, $c' = 80$ kPa and $\gamma = 19.6$ kN/m³. There appears to be some confusion over these parameters, because also in the published paper, it is stated that the reinforcement layout was designed using Jewell's Charts, which do not include c' . However c' is very high as stated, and does not appear to represent true drained shear strength, especially for a fill which would be expected to have a very low c' component. Using $\phi' = 29^\circ$, $c' = 0$ kPa for the fill results in F well below 1.0, even for the stated design accelerations of $A_h = A_v = 0.15g$. Despite these discrepancies, the reported fill strength parameters have still been used in the analysis presented below for the sake of consistency, being the properties used at the time of design. The slope is reinforced with HDPE geogrid, consisting of a single grade with tensile strength of 100 kN/m and a vertical spacing of 0.5m over the full height of the slope.

Bench	Static	$A_h = 0.15g$ $A_v = 0.15g$	$A_h = 0.3g$	$A_h = 0.3g$ $A_v = 0.15g$	$A_h = 0.4g$
Base	1.784	1.357	1.182	1.156	1.036

Table 3 Minimum factors of safety calculated for the Nantou slope for varying peak ground accelerations.

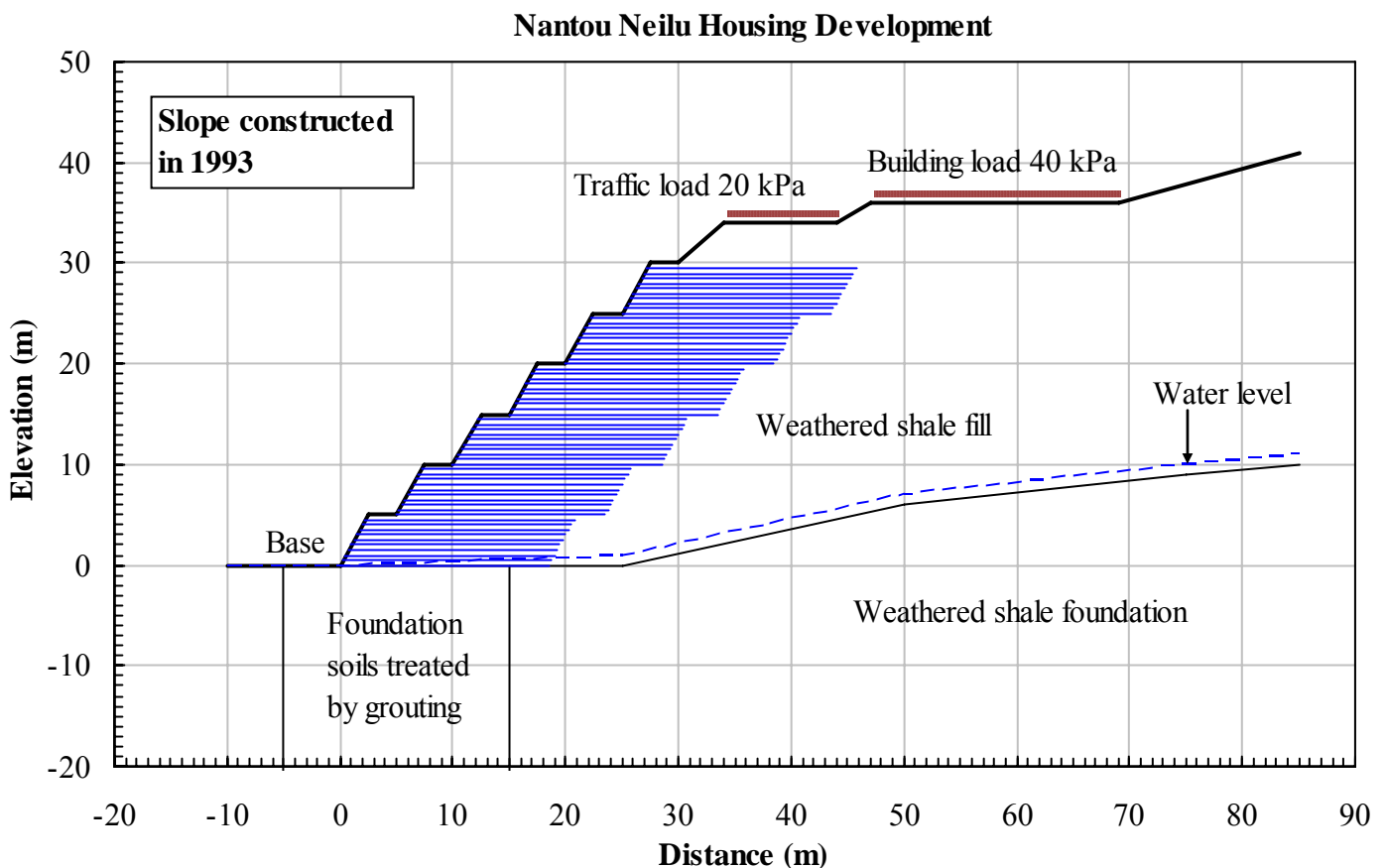


Figure 13. Typical cross section of the Nantou reinforced soil slope.

Stability analyses have been carried out using the Winslope program, and the results are summarised in Table 3. Because the reinforcement layout consists of a single reinforcement type of uniform length and spacing, only circles passing through the base are included in Table 3 (in fact the upper part of this slope has a very high factor of safety, and it is actually considerably over-designed near the top). The sensitivity of the results to peak ground acceleration is again examined by using the same acceleration values as applied to the Fengyuan slope, up to the maximum recommended for pseudo-static analysis of 0.4g. At the time of the Chi-

Chi earthquake, there were no houses built above the slope, so that the surcharges were omitted for accelerations of 0.3g and higher in Table 3.

The critical peak ground acceleration (ie ground acceleration resulting in $F = 1.0$) is around $A_h = 0.4g$. As with Fengyuan, the slope at Nantou survived the Chi-Chi earthquake without any visible damage, and the analysis outlined above compared to the likely level of ground motions suggested on Figure 10 indicates that this could have been expected based on routine stability analysis.

4.5 Slope at Chi-Nan University

The slope at Chi-Nan is situated about 27 km from the fault break, and about 18 km from the epicentre. The slope failed dramatically during the earthquake and has received much attention from researchers since. Information summarised here is taken from Huang (2000), Chou and Fan (2001) and Holtz et al (2001). The slope was built between 1994 and 1996, suffering some stability problems during and soon after construction. The slope was required to help stabilise a steepened cutting, permitting construction of an access road to the university. Therefore one major difference between this slope and the other two described above is that it was built against a cutting into existing soil whereas the other two were in zones of fill only. Peak ground accelerations recorded at a nearby seismograph station (Puli, TCU074) were $A_h = 0.59g$ and $A_v = 0.27g$.

A typical cross section of the slope is shown on Figure 14. The reinforced section is 40m high with face angle 0.5:1 and 3m wide benches every 10m. There are a number of lower angle unreinforced benches above the reinforced section, cut into the existing soils, as well as a 10m high bench below it which supports the reinforced section and is referred to here as the foundation. The fill soils used for the construction are described as lateritic gravel with clay infill, consisting of soils taken from the cutting during construction. Parameters given for the fill by Chou and Fan (2001) are $\phi' = 30^\circ$, $c' = 48$ kPa and $\gamma = 20$ kN/m³. Of greater importance to stability in this case are the parameters of the existing soils, given as $\phi' = 39^\circ$, $c' = 40$ kPa and $\gamma = 20$ kN/m³ for the upper gravel and $\phi' = 39^\circ$, $c' = 70$ kPa and $\gamma = 21$ kN/m³ for the lower gravel. All these values are characterised by very high c' , however analysis of the cutting during construction requires that parameters of this order are used to ensure temporary stability of the cut slope under static conditions. These values are used in the analysis summarised here. The slope is reinforced with polyester geogrid, consisting of two grades, with tensile strength of 104 kN/m in the lower bench and 60 kN/m for the upper three benches, all with a vertical spacing of 1.0m. Based on test data summarised by Holtz et al, these appear to be long term strengths.

Bench	Static	$A_h = 0.15g$ $A_v = 0.15g$	$A_h = 0.3g$	$A_h = 0.3g$ $A_v = 0.15g$	$A_h = 0.4g$
Base	1.262	1.081	0.881	0.860	0.764
Fdn	1.376	1.115	0.903	0.881	0.783

Table 4 Minimum factors of safety calculated for the Chi-Nan slope for varying peak ground accelerations.

Stability analyses have been carried out using the Winslope program, and the results are summarised in Table 4. As noted by Holtz et al (2001), failure took place along the boundary between the reinforced soil zone and the original slope, so that for a full *back-analysis*, slip circles would not be appropriate. However, as stated at the end of Section 4.2, the aim of this analysis is to establish if instability could have been anticipated from routine stability calculations. Circles passing through the base are included in Table 4, as well as through the foundation. Before failure, the lower unreinforced bench had a pattern of concrete beams on the surface, possibly connected to anchors, but after the failure, the author noted that these beams had been displaced outwards and downwards and were resting on the road, implying a failure through the foundation. The sensitivity of the results to peak ground acceleration is again examined by using the same acceleration values as applied to the Fengyuan slope, up to the maximum recommended for pseudo-static analysis of 0.4g.

From the results in Table 4, it can be seen that for the static condition and lower values of ground acceleration, the slope could be expected to remain stable (values of F similar to those published by Huang, 2000, with slightly different soil parameters), however for $A_h = 0.3g$ and above, the factor of safety drops to values below 0.8, so that the observed instability might have been anticipated for such high peak accelerations (even though the circular failure mechanism is not what actually happened). Holtz et al concluded that one of the main contributors to the observed instability of this slope was the very short length of the reinforcement (13m in the lowest bench reducing to only 4m in the top bench), and as can be seen by comparing the three sections, this is one of the important differences between the Chi-Nan slope and the other two which did not fail.

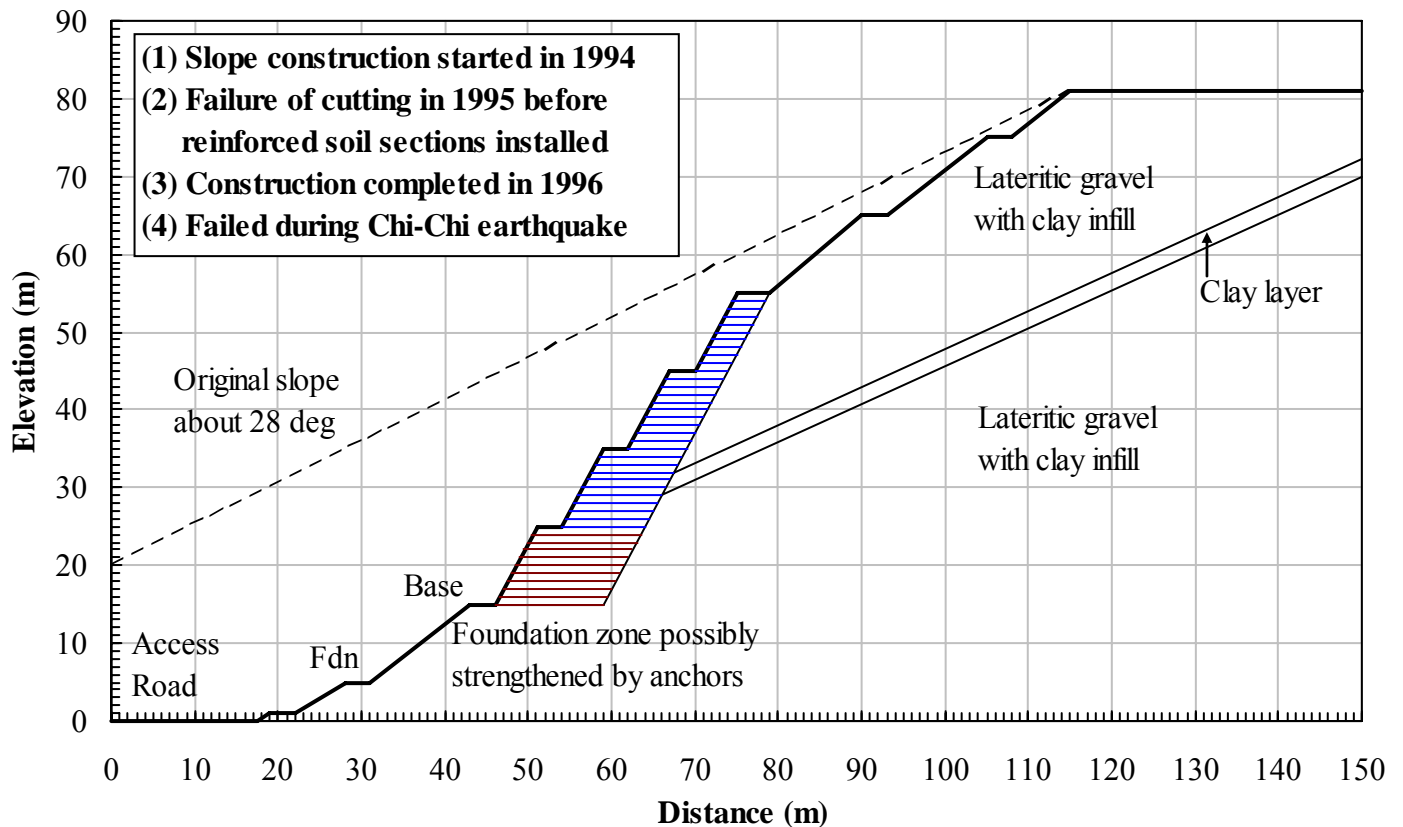


Figure 14. Typical cross section of the Chi-Nan reinforced soil slope.

5 CONCLUSIONS

- Bishop's simplified method of slices using a circular arc may be adapted to include both the destabilising effect of earthquake loading and the stabilising effect geosynthetic reinforcement. Various important features and parameters may be included in the analysis, which define both the ground accelerations from an earthquake and the resistance from the reinforcement appropriate to this situation.
- Application of this method of analysis using a suitable computer program to three large reinforced soil slopes affected by the 1999 Chi-Chi earthquake indicates that the observed behaviour could have been expected (one slope failed and two remained stable), based on routine design calculations.
- In fact the actual peak ground accelerations at these three sites may well have been higher than the upper limit of 0.4g recommended for pseudo-static analysis, so that the observed behaviour of the three reinforced soil slopes demonstrates that the proposals for seismic design presented in this paper are conservative, provided that the vertical component of acceleration is included in the analysis.
- The circular slip analyses summarised above, including data entry and examining sensitivity to various parameters, took no more than two hours each to carry out. Therefore with a suitable computer program, time is not a barrier to carrying out thorough analysis of such structures. However it should be added that other possible modes of failure (apart from slip circles) should also be checked, such as sliding on the base of the structure and two-part wedge mechanisms.
- Significant vertical accelerations are a characteristic of many major seismic regions, which tend to be associated with subduction zones. Only in locations in which shearing is predominantly translational, such as California, is this not the case. An understanding of the effect of vertical accelerations is therefore essential for meaningful seismic slope stability analysis.
- It is finally concluded that an adequately designed reinforced soil slope has excellent resistance to strong ground shaking during an earthquake, even when design ground accelerations are very high. However use of sensible minimum L/H ratios (ratio of length of reinforcement to height of slope) of is an important requirement.

ACKNOWLEDGEMENT

I am greatly indebted to Chris Jenner of Tensar International and Paul McCombie of the University of Bath, for their review and comments on this paper, as well Paul's many years of dedicated work in developing the Winslope computer program.

REFERENCES

- Bathurst R J. Segmental retaining wall seismic design procedure. National Concrete Masonry Association (NCMA), Supplement to design manual for segmental retaining walls, 2nd Edition, Virginia, USA, 1998.
- Bishop, A. W. The use of the slip circle in the stability analysis of slopes. *Geotechnique*, Vol. 5, No. 1, pp 7-17, 1955.
- Cai, Z. and Bathurst R J. Seismic induced permanent displacement of geosynthetic reinforced segmental retaining walls. *Canadian Geotechnical Journal*, Vol. 33, pp 937-955, 1996.
- Chao, N. N. S., Hew, J. H. C. and Rimoldi, P. 35m high geogrid-reinforced slope: new heights and innovative construction. *Proceedings 5th International Conference on Geotextiles, Geomembranes and Related Products*, pp 473-477, Singapore, 1994.
- Chou, N.S. and Fan, C.C. Dynamic simulation of the reinforced soil slope failure at the Chi-Nan University during the 1999 Chi-Chi earthquake. *Proceedings International Geosynthetic Engineering Forum*, pp 111-124, Taipei, Taiwan, 2001
- Elias, V., Christopher, B. R. and Berg, R. R. Mechanically stabilised earth walls and reinforced soil slopes design and construction guidelines. Report No. FHWA-NHI-00-043, Federal Highway Administration, Washington DC, USA, 2000.
- Holtz, R.D., Kramer, S.L., Hsieh, C.W., Huang, A.B., and Lee, W.F. Failure Analysis of an 80m High Geogrid Reinforced Wall in Taiwan. *Proceedings, XVth International Conference on Soil Mechanics and Geotechnical Engineering*, Istanbul, Turkey, Vol. 2, pp 1159-1162, 2001
- Huang, C. C. Investigations of soil retaining structures damaged during the Chi-Chi (Taiwan) earthquake. *Journal of the Chinese Institute of Engineers*, Vol. 23, No. 4, pp 417-428, Taiwan, 2000.
- Idriss, I. M. and Abrahamson N. A. Geotechnical aspects of the earthquake ground motions recorded during the 1999 Chi-Chi Earthquake. Keynote Session C, *Proceedings, International Workshop on the Annual Commemoration of the Chi-Chi Earthquake*, National Center for Research on Earthquake Engineering (NCREEE), Volume III, pp 9 – 22, Taipei, Taiwan, 2000.
- McCombie, P. F. Notes on development of the Tensar International computer program "Winslope". Internal document, Tensar International, 2006.
- McGown, A. The behaviour of geosynthetic reinforced soil systems in various geotechnical applications. Mercer Lecture, 2000.
- Wood, J. H. and Elms, D. G. Seismic design of bridge abutments and retaining walls. *RRU Bulletin 84*, Vol 2, Transit New Zealand, Wellington, 1990.